TISSUE ENGINEERING: Part A
Volume 30, Numbers 7 and 8, 2024

DOI: 10.1089/ten.tea.2023.0110

termis
Tissue Engineering
& Regenerative Medicine
International Society

SPECIAL ISSUE: MODULATION OF THE IMMUNE SYSTEM

Macrophage Mechano-Responsiveness Within Three-Dimensional Tissue Matrix upon Mechanotherapy-Associated Strains

Parto Babaniamansour, MSc,[1] Diego Jacho, MSc,[1] Ashley Teow, MSc,[1] Agustin Rabino, BSc,[2] Rafael Garcia-Mata, PhD,[2] and Eda Yildirim-Ayan, PhD[1]

Mechano-rehabilitation, also known as mechanotherapy, represents the forefront of noninvasive treatment for musculoskeletal (MSK) tissue disorders, encompassing conditions affecting tendons, cartilage, ligaments, and muscles. Recent emphasis has underscored the significance of macrophage presence in the healing of MSK tissues. However, a considerable gap still exists in comprehending how mechanical strains associated with mechanotherapy impact both the naïve and pro-inflammatory macrophage phenotypes within the three-dimensional (3D) tissue matrix, as well as whether the shift in macrophage phenotype is contingent on the mechanical strains inherent to mechanotherapy. In this study, we delineated alterations in mechano-adaptation and polarization of both naive and M1 macrophages within 3D matrices, elucidating their response to varying degrees of mechanical strain exposure (3%, 6%, and 12%). To evaluate macrophage mechano-adaptation and mechano-sensitivity within 3D collagen matrices under mechanical loading, we employed structural techniques (scanning electron microscopy, histology), quantitative morphological measures for phenotypic assessment, and genotypic methods such as quantitative real-time polymerase chain reaction. Our data reveal that the response of macrophages to mechanical loading is not only contingent on their specific sub-phenotype but also varies with the amplitude of mechanical strain. Notably, although supra-mechanical loading (12% strain) was requisite to induce a phenotypic shift in naive (M0) macrophages, as little as 3% mechanical strain proved sufficient to prompt phenotypic alterations in pro-inflammatory (M1) macrophages. These findings pave the way for leveraging the macrophage mechanome in customized and targeted applications of mechanical strain within the mechano-therapeutic framework. Considering the prevalence of MSK tissue injuries and their profound societal and economic implications, the development of well-informed and effective clinical mechanotherapy modalities for MSK tissue healing becomes an imperative endeavor.

Keywords: cytoskeleton, inflammation, immunomodulation, macrophage polarization, macrophage-laden 3D matrix, mechanotherapy, mechanotransduction, musculoskeletal tissue regeneration

Impact Statement

Mechanotherapy is a primary noninvasive treatment for musculoskeletal (MSK) tissue injuries, but the effect of mechanical strain on macrophage phenotypes is not fully understood. A recent study found that macrophage response to mechanical loading is both sub-phenotype specific and amplitude-dependent, with even small strains enough to induce phenotypic changes in pro-inflammatory macrophages. These findings could pave the way for using macrophage mechanome in targeted mechanotherapy applications for better MSK tissue healing.

Departments of [1]Bioengineering and [2]Biological Sciences, University of Toledo, Toledo, Ohio, USA.

Introduction

Nearly 35 million musculoskeletal (MSK) injuries are reported each year only in the United States, with an annual cost of around $30 billion.[1–3] A convincing body of clinical evidence state that innate immune cells, including macrophages, are critical regulators in MSK tissue regeneration.[4–9] On injury, the circulating blood monocytes extravasate into the tissue and differentiate into naive macrophages (M0), which concomitantly differentiate into classically activated macrophages (M1) to stimulate the precursor cell proliferation through the secretion of pro-inflammatory molecules, including tumor necrosis factor (TNF)-α, interleukin (IL)-6, and IL-1β in the gene expression section and phagocyte the tissue debris.

Following the initial inflammatory phase, macrophages can alter their metabolic functions and polarize from a pro-inflammatory phenotype to a healing/growth-promoting phenotype (M2).[7,10,11] These sequential and also transient phenotypic changes in macrophages either contribute to or hinder MSK tissue regeneration depending on the microenvironment circulating the macrophages.[12–14]

The nonsteroidal anti-inflammatory drugs (NSAIDs) are commonly used with MSK injuries because of their immunomodulatory effects on activated macrophages and, subsequent, therapeutic effect against inflammatory symptoms.[15–17] Despite this, the recent *in vivo* and clinical data indicate that NSAIDs can impair MSK tissue healing,[18–20] weaken MSK tissue mechanical stability,[21–23] and lead to spontaneous post-injection ruptures in connective MSK tissues.[24]

Thus, mechanotherapy exercises (physical therapy), which are already frequently employed in clinical settings, become prominent noninvasive treatment strategies for MSK tissue healing. The MSK tissues require mechanical loading for hemostasis and recovery.[17] *In vitro*, [25,26] *in vivo*, [27,28] and silico models[29–33] demonstrated that in the absence of mechanical loading, the strength of MSK tissue decrease while inflammatory response increases.[34,35]

For instance, the recent *in vivo* mechanotherapy studies highlight the importance of early mobilization and mechanical loading in tendon tissue healing.[36] The 15 min of mechanical loading from as early as 3 days after injury were sufficient to increase callus thickness and strength of the healing tendon.[9,37] These studies demonstrate the importance of mechanical loading on MSK tissue regeneration; however, the macrophage mechanome governing the inflammation still remains unknown.

It is often thought that mechanical loading during mechanotherapy exercises mainly affects the extracellular matrix (ECM) formation and remodeling,[17] yet it was recently reported that mechanical loading first affects the early inflammatory phase of healing by modulating the macrophage polarization and then subsequently affects MSK tissue regeneration. The recent *in vivo* mechanotherapy studies demonstrated the interaction of mechanical loading and inflammation around the injured MSK tissue.

On mechanotherapy exercises as short as 30 min/day for 5 days, the pro-inflammatory gene (IL-1β, TNF-α, interferon-gamma [IFN-γ]) expressions were significantly down-regulated on the mechanically loaded MSK tissue (tendon) compared with immobilized counterparts using botulinum toxin A (Botox) injection.[38] Thus, it is important to understand how mechanical loadings associated with mechanotherapy exercises modulate the macrophage phenotype toward pro-inflammatory lineages, which is a crucial step toward tissue regeneration.

Yet, the adaptive phenotypic response of macrophages to mechanical loading, unloading, and overloading is not fully understood. Toward this end, the objective of this study is two-fold: (a) to understand how various mechanical loading amplitudes utilized in mechanotherapy exercises affect naive (M0) and pro-inflammatory macrophage (M1) polarization on their extravasation within the three-dimensional (3D) tissue; (b) to understand the mechano-responsiveness of macrophage sub-phenotypes to the same mechanical loading condition and whether the macrophage mechano-responsiveness is phenotype-specific.

Materials and Methods

Macrophage cultivation

The human pro-monocytic cell line U937 (ATCC, VA, USA) was cultured in Roswell Park Memorial Institute (RPMI) 1640 medium (ATCC), supplemented with 10% (v/v) heat-inactivated fetal bovine serum (ThermoFisher, USA), 2 mM L-glutamine, 10 mM HEPES, 1 mM sodium pyruvate, 4500 mg/L glucose, and 1500 mg/L sodium bicarbonate and kept in the incubator (37°C, 5% carbon dioxide) for expansion.

After changing the medium every 2–3 days and on reaching confluency, the U937 monocyte cells were treated with 100 ng/mL of phorbol 12-myristate 13-acetate (PMA; Sigma-Aldrich, USA) for 24 h to be differentiated into naive macrophages (M0). Different PMA concentrations and incubation times were tested based on cell viability (data not shown). As a result, 24 h incubation with 100 ng/mL of PMA was selected to differentiate blood-derived monocytes to naive macrophages.

To polarize M0 macrophages to pro-inflammatory (M1) phenotype, the cells were further cultured within the media supplemented with 20 ng/mL IFN-γ (Peprotech, Cranbury, NJ) and 100 ng/mL lipopolysaccharide (LPS; Sigma, USA) for 24 h. Moreover, to polarize M0 macrophages to anti-inflammatory (M2) phenotype, the cells were further cultured within the media supplemented with 100 ng/mL IL-4 (Peprotech) for 24 h.

Macrophage phenotype assessment before macrophage-laden 3D tissue matrix synthesis

Before encapsulating macrophages within the 3D tissue matrix and applying mechanical stimulation, the phenotype of monocyte-derived naive macrophages (M0) and classically activated macrophages (M1) was confirmed using immunofluorescence staining. Briefly, 24 h after PMA treatment, cells were fixed in 4% paraformaldehyde and then quenched with ammonium chloride for 15 min each. Then, cells were permeabilized with Triton X-100 for 15 min and washed in phosphate-buffered saline (PBS).

Subsequently, cells were incubated for 20 min with 2.5% (v/v) goat serum (Invitrogen) and 0.2% Tween Solution in PBS to block non-specific antibody binding. After blocking, cells were incubated overnight at 4°C in mouse CD80

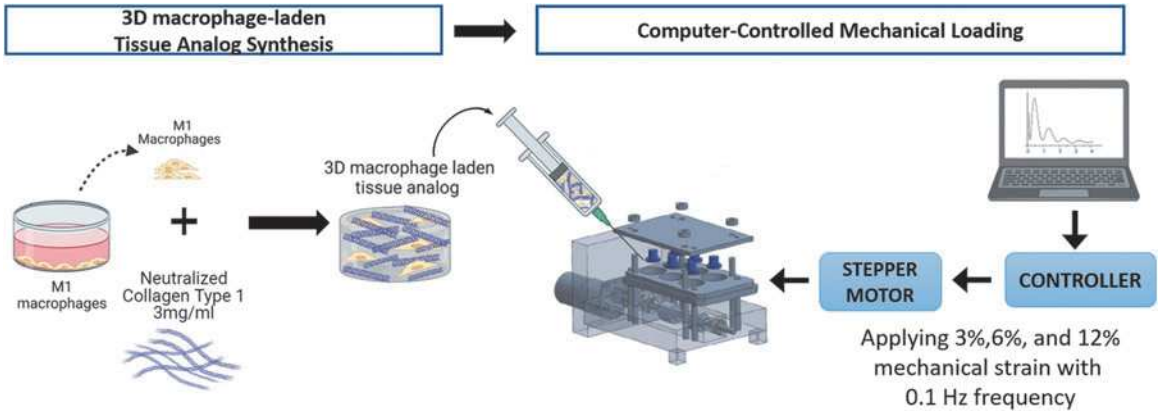

FIG. 1. Schematic representations of synthesizing macrophage-laden 3D tissue matrix and computer-controlled mechanical loading of macrophage-laden matrix using custom-built mechanical loading platform. 3D, three-dimensional.

antibody (1:100; TA501575; Invitrogen) and rabbit CD206 antibody (1:100; MA1-35936; ThermoFisher).

The following day, cells were washed three times with PBS and 0.2% Tween solution and blocked in 0.4% bovine serum albumin and 0.2% Tween solution for 20 min at room temperature. Subsequently, samples were incubated with goat anti-rabbit IgG (H + L) Secondary Antibody Alexa Fluor 596 (1:1000; A32740; ThermoFisher), goat anti-mouse IgG (H + L) Secondary Antibody Alexa Fluor 647 (1:1000; A32828; ThermoFisher), and Alexa Fluor 488 Phalloidin (1:50; A12379; ThermoFisher) for 3 h.

Finally, cells were incubated with 4′,6-Diamidino-2-Phenylindole (DAPI; Life Technologies, USA) dye (1:1000) in PBS for 30 min, washed with 0.2% tween, and mounted on glass slides. Samples were imaged using a 63× oil or 20× airy objective with a Leica Stellaris 5 confocal system equipped with HyD detectors and the LASX software.

Confocal images from at least three independent studies were processed to visualize each cell's nuclei, filamentous actin (F-actin), and M1 and M2 phenotypic expression ($n = 3$). To quantify F-actin density, the confocal images of M0 and M1 macrophages stained with Alexa Fluor 488 Phalloidin were post-processed, analyzed, and normalized using ImageJ. In total, 30 cells from each image with 5 different fields of view were processed for each group. Each cell was segmented using both signals (DAPI and F-actin).

For normalization, all image stacks of each field of view were merged into a single composite image and subsequently normalized by subtracting the background noise from the composite image. The integrated density of each cell was obtained and then divided by the cell area to report F-actin per unit area for each cell. The quantified data were plotted using the individual data point plot.

Similarly, the expression of the pro-inflammatory marker (CD80) and the anti-inflammatory marker (CD206) was quantified to determine the integrated density values, which were subsequently adjusted by subtracting the background signal. The resultant integrated density value was then normalized by the cell's surface area to ascertain the signal intensity attributed to the CD80 and CD206 markers, respectively.

This article showcased the expression of CD80 and CD206 in M1 macrophages as discrete data points, highlighting the prevalence of pro-inflammatory markers over anti-inflammatory markers. In addition, the presentation of CD206 expression in both M1 and M2 macrophages served as individual data points, emphasizing the prevalence of anti-inflammatory markers in M2 macrophages in contrast to M1 macrophages.

Synthesizing macrophage-laden 3D tissue matrix and applying mechanical loading

After confirming monocyte-derived naive macrophage (M0) and pro-inflammatory macrophage (M1) phenotypes, the M1 or M0 macrophages were encapsulated with the neutralized 3 mg/mL collagen type-1 (Corning, USA) with 1×10^6 cells/mL seeding density using our established protocols.[39,40] Collagen type-I was chosen as a tissue matrix material since most MSK tissue ECM comprises collagen type-I.[41]

Then, macrophage-laden 3D tissue matrices were deposited into the mechanical loading apparatus and incubated for 2 h for collagen polymerization. Following a 2-h incubation, the complete RPMI-1640 media was added to the macrophage-laden 3D tissue matrices and incubated for 24 h for acclamation before mechanical loading. Figure 1 demonstrates the significant steps for cell cultivation and macrophage-laden tissue matrix synthesis.

Following a 24-h incubation, the various mechanical strains with 3%, 6%, or 12% amplitudes and 0.1 Hz frequency were applied to the 3D tissue matrix with macrophages using our well-established and computer-controlled mechanical loading platform called EQUicycler (Fig. 1). The EQUicycler can culture *ex vivo* intervertebral disk (IVDs) and 3D cell-laden MSK tissue scaffolds under various mechanical strain amplitudes up to 15% at different frequencies (up to 2 Hz) without creating damage in cell-laden tissue constructs or the *ex vivo* IVDs.[39,42,43,]

The EQUicycler generates cyclic or static vertical displacements in the moving plate against the 3D scaffolds hosted in the fixed plate. A precise moving plate displacement corresponding to a predefined strain was calculated using finite element analysis and was input as a number of steps to the stepper motor. The stepper motor and the motion frequency were controlled by a controller (Lin Engineering,

USA) using a custom-built LabVIEW-based coding to define various mechanical strains and frequencies based on the application area.[44]

The mechanical strain amplitudes and frequency were chosen to mimic the physiological strain applied on the MSK tissue.[26,45] Based on the normal physiological range that MSK tissues can undergo, the experiment was devised to subject the tissues to 3%, 6%, and 12% strains, representing low, moderate, and high strain levels, respectively, to establish a physiologically relevant model.

The mechanical loading was conducted for 2 h a day for 7 days. The 0% mechanical strain group was used as a control. On completion of mechanical loading, the 3D tissue matrix encapsulating macrophages was harvested for structural, cellular, and molecular characterizations.

Structural changes in 3D macrophage-laden tissue matrix on mechanical loading

Structural changes in naive- and pro-inflammatory macrophage-laden tissue matrix were assessed on mechanical loadings using scanning electron microscopy (SEM) and histology images analyses. For SEM analysis, after 7 days of mechanical loading, the macrophage-laden tissue matrices were removed from the mechanical loading platform and fixed overnight with 4% paraformaldehyde.

Subsequently, the matrices were dehydrated within a series of ethanol/water incubation ranging from 30% to 100%. The matrices were then soaked into a series of hexamethyldisilane (ThermoFisher)/ethanol gradients ranging from 30% to 100% for image clarity. Before SEM imaging, the matrices were air-dried overnight under the chemical hood and gold sputter coated. The SEM images were then analyzed using ImageJ (NIH, USA) and Nearest distance plugging to understand the changes in collagen fiber organization, fiber diameters, and matrix porosity for M0- and M1-laden tissue matrices exposed to various mechanical strain amplitudes.

Four images from each mechanical strain group were used in fiber diameter and porosity calculations. The ratio between the total area and the area of pores in the matrix calculated the percent porosity. After completing 7 days of mechanical loading for histology analysis, the M0- and M1-laden tissue matrices were first washed with 1×PBS and then submerged in 10% formalin.

Then, they were dehydrated via an ethanol gradient and cleared with xylene to be ready for paraffin embedding. The tissue matrices were sliced at a thickness of 5 μm using a microtome (GMI-Reichert Jung 820 II) and mounted on a glass microscopic slide to be stained with Masson's Trichrome for collagen fibers.

Viability of macrophages within 3D tissue matrix on mechanical loading

Following 7 days of mechanical loading with different amplitudes, the viability of naive and pro-inflammatory macrophages was evaluated using a Live-Dead Assay kit (Life Technologies). On characterization day, the cell-laden 3D tissue matrices were incubated with Dulbecco's modified Eagle medium supplemented with 4 μM calcein AM and 8 μM ethidium homodimer-1 dyes (1:4 ratio) for 2 h at 37°C.

The 3D tissue matrices were then fixed with 4% paraformaldehyde (Sigma) for another 30 min at room temperature and washed thoroughly with dPBS. Then, the 3D constructs were transferred to an 8-well μ-slide glass bottom (Ibidi, USA) and covered with 200 μL of mounting media (Permount, USA). Slides were imaged with a 63× oil, 1.4 NA or 20× dry, 0.75 NA objective with an Andor Dragonfly 200 spinning disk confocal microscope mounted to a Leica DMi8 microscope and Fusion software as described in our previous protocol.[40]

The live cells were green at 490/525 nm excitation/emission wavelengths, whereas the dead cells were red at 557/576 nm excitation/emission wavelengths. The confocal images were then analyzed using Image J (NIH) to assess how mechanical loading affected the cell viability within the 3D tissue matrix. For quantitative analysis, the 50 μm z-stacks were analyzed for background removal, and particle analysis was carried out in each channel.

Then, the number of live cells in each z-stack was counted. At least three fields of view from each sample were analyzed, and 150 cells per group were analyzed. The total number of cells in each z-stack was used to extrapolate the number of cells in sample. Cell proliferation was assessed by comparing the initial (day 0) number of live cells with the number of live cells on the day of characterization.

Phenotypic changes in macrophage within 3D tissue matrix on mechanical loading

Following 7 days of mechanical loading, the quantitative real-time polymerase chain reaction (qRT-PCR) was performed to assess the changes in the expression of pro-and anti-inflammatory genes expressed by M0 and M1 macrophages. Briefly, on characterization day, the M0- and M1-laden matrices were retrieved from EQUicycler chambers. Then, RNA was extracted using TRIzol reagent (ThermoFisher Scientific).

The isolated RNA was reverse transcribed using the Omniscript RT kit (Qiagen, USA) per the manufacturer's instructions. The qRT-PCR was performed using the SYBR Green PCR master mix (ThermoFisher Scientific) to detect the expression of pro- and anti-inflammation hallmark markers. The relative fold changes between control (0% mechanical loading) and 3%, 6%, and 12% mechanical strain applied macrophage-laden matrices were obtained using the ΔΔCt method.

The ΔΔCt method used glyceraldehyde-3-phosphate dehydrogenase (*GAPDH*) as the housekeeping normalizing gene. The qRT-PCR was performed in iCycler iQ detection system (Bio-Rad, USA), with thermocycling performed for 35 cycles. The primer sequences were obtained from published literature, as listed in Table 1, and purchased from Integrated DNA Technologies (USA).

Based on fold change values of pro- and anti-inflammatory genes, the heatmaps were generated using open-source software (http://www.heatmapper.ca) to facilitate the pattern discovery in each strain group by visual inspection. Each heatmap was created based on the average linking method combined with the Spearman Rank Correlation method.

Statistical analysis

Six samples ($n=6$) were used for all assays, and the statistical analysis was done through RStudio. Statistical

Table 1. Forward and Reverse Primers for Quantitative Real-Time Polymerase Chain Reaction

Gene	*Forward primer*	*Reverse primer*	*Reference*
c-Fos	5′-CTTTGCAGACCGAGATTGCC-3′	5′-CTTTGCAGACCGAGATTGCC-3′	47
MMP3	CAGCCAACTGTGATCCTGCT	CTTCATATGCGGCATCCACG	41
TNF-α	5′-AGAGGGAAGAGTTCCCCAGGGAC-3′	5′-TGAGTCGGTCACCCTTCTCCAG-3′	48
IL-1β	5′-CCAGCTACGAATCTCGGACCACC-3′	5′TTAGGAAGACACAAATTGCATGGTGAAGTCAGT-3′	49
CD163	5′-TCTGTTGGCCATTTTCGTCG-3′	5′TGGTGGACTAAGTTCTCTCCTCTTGA-3′	48
CCL18	5′-AAGAGCTCTGCTGCCTCGTCTA-3′	5′-CCCTCAGGCATTCAGCTTAC-3′	50
IL-10	5′-CCTGTGAAAACAAGAGCAAGGC-3′	5′-TCACTCATGGCTTTGTAGATGCC-3′	48
GAPDH	5′-AGAAGGCTGGGGCTCATTTG-3′	5′-AGGGGCCATCCACAGTCTTC-3′	50

significance was conducted using one-way analysis of variance and *post hoc* analysis (Tukey test) or Student's *t*-test where appropriate. (*) represents a significant difference in all groups compared with the control, (#) represents a significant difference between 3% and 6% strain groups, (§) represents a significant difference between 6% and 12% strain groups, and (†) represents a significant difference between 3% and 12% strain groups, each with a 0.05 *p*-value. Double symbol (**, ##, §§ and ††) shows that the significance level in statistical analysis between the groups is $p < 0.005$ instead of $p < 0.05$. In graphs, the error bars represent the standard deviations unless otherwise specified.

Results

Confirming phenotypic changes in naive and pro-inflammatory macrophages

Before conducting extensive cellular and structural analysis with M0- and M1-laden 3D collagen tissue matrices on mechanical loading, the phenotypic characterization was conducted for monocyte-derived naive macrophages (M0) and classically activated macrophages (M1) using immunofluorescence staining.

Figure 2 demonstrates the immunofluorescence images of M0 and M1 cells tagged with *CD80* and *CD206* antibodies, phalloidin, and DAPI staining. In addition, M2 macrophages were tagged with CD206 as a positive control for anti-inflammatory phenotypic assessment.

Following PMA treatment, the non-adherent monocytes became M0 macrophages and adhered to the surface. The phalloidin staining of M0 macrophages demonstrated filamentous actin (F-actin) formation, which is essential for adhesion. For naive (M0) macrophages, CD206 and CD80 surface proteins were not observed in immunofluorescence images (Fig. 2, first row).

M0 macrophages were then differentiated into M1 macrophages through incubating them with 100 ng/mL LPS and 20 ng/mL IFN-γ for another 24 h. The M1 differentiation was confirmed with the robust expression of CD80 surface protein, which is a prominent classically activated macrophage indicator.[46,47] Individual data points plot in Figure 2A shows that the average signal intensity of CD80 (62.52 ± 27.06) is significantly higher ($p < 0.005$) than the average signal intensity of CD206 (47.34 ± 22.44).

For CD206, the Mannose receptor and an important anti-inflammatory marker, the fluorescence signal was negligible in M1 macrophages compared with their counterparts in M2 (anti-inflammatory) macrophages. Individual data points plot in Figure 2B shows that the average signal intensity of CD206 in M1 macrophages (47.34 ± 22.44) is significantly lower ($p < 0.005$) than the average signal intensity of CD206 in M2 macrophages (82.48 ± 58.12).

Cell viability of M0 and M1 macrophages within 3D tissue matrix on mechanical loading

The effect of mechanical loading with different amplitudes (0%, 3%, 6%, and 12% strain) on the viability of M0 and M1 macrophages within the 3D matrix was assessed by live/dead double staining (Fig. 3).

For M0-laden matrices, the number of M0 macrophages increased significantly ($p < 0.05$) with the increased mechanical strain compared with the control (0%) group (Fig. 3C). Even the supra-mechanical loading (12%) applied on M0-laden matrices did not create cell death for M0 macrophages residing within the 3D matrix. In fact, the M0-laden matrices that were subjected to 12% mechanical strain demonstrated an almost 4.8-fold increase in the number of live cells over 7 days of stimulation compared with the non-loaded samples (0% strain).

The effect of mechanical loading was different on M1 macrophages than the M0 macrophages. For M1 macrophages, although no significant cell death was observed with the increased mechanical loading (Fig. 3B), the total number of M1 macrophages were significantly less compared with M0 cells for all mechanically loaded groups (Fig. 3C). Figure 3C shows that on 7 days of mechanical stimulation, the number of M0 macrophages increased around 4-fold, 11-fold, 8-fold, and 18-fold in 0%, 3%, 6%, and 12% mechanical stimulation groups, respectively.

However, the number of M1 macrophages increased around 5-fold, 4-fold, 6-fold, and 4-fold in 0%, 3%, 6%, and 12% mechanical stimulation groups, respectively. Therefore, M1 macrophages did not proliferate as much as M0 macrophages during the culture period. This can be attributed to the additional *LPS* and *IFN-γ* treatment of M1 macrophages, which might affect the proliferation capacity of the M1 cells.

Structural changes in macrophage-laden 3D collagen tissue matrix on mechanical loading

The structural changes of M0- and M1-laden 3D tissue matrix on 0%, 3%, 6%, and 12% mechanical strain were visualized and assessed using SEM and histology images (Fig. 4). Figure 4A and 4B demonstrate the SEM images of M0- and M1-laden tissue matrices, whereas Figure 4C shows the changes in matrix fiber diameter with the increased mechanical strains.

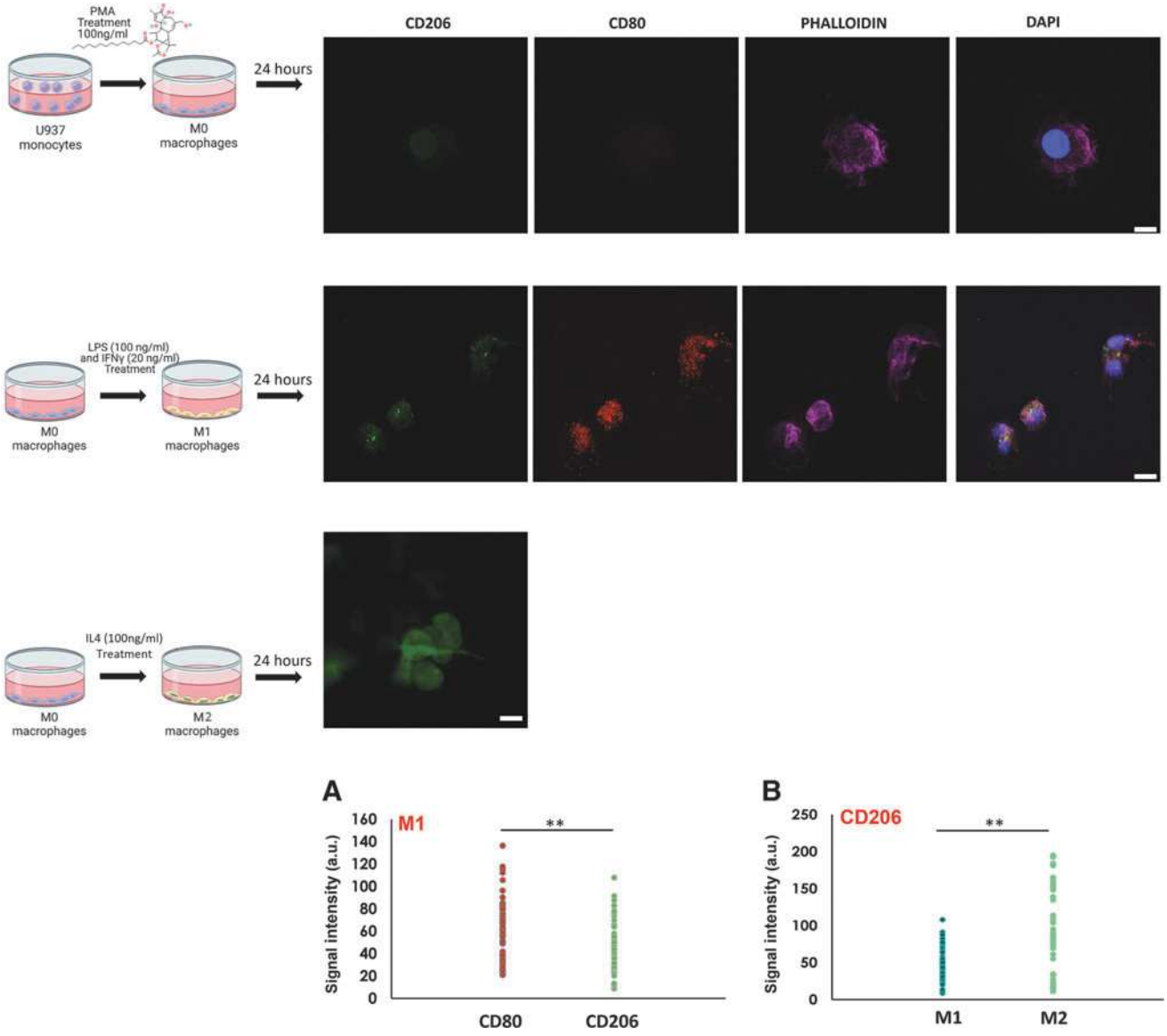

FIG. 2. Immunofluorescence staining of M0 and M1 macrophages with CD206 (*green*) as an M2 marker, CD80 (*red*) as an M1 marker, Alexa Fluor 488 Phalloidin (*purple*) as an F-actin staining, and DAPI (*blue*) for the cell nucleus. The M2 macrophages were stained with CD206 as a control. In all images, the scale bar is 10 μm. **(A)** represents the individual data point plot comparing the expression of CD80 and CD206 in M1 macrophages. **(B)** represents the individual data point plot comparing the expression of CD206 in M1 and M2 macrophages. **indicates significant difference between M0 and M1 macrophages, with a $p < 0.005$. DAPI, 4′,6-diamidino-2-phenylindole.

Figure 4D shows Masson's trichrome staining of M1-laden matrix on 0%, 3%, 6%, and 12% mechanical strain exposure. For M0-laden tissue matrix, the SEM images (Fig. 4A) and fiber diameter analysis (Fig. 4C) revealed that there was no statistical ($p < 0.05$) difference in fiber diameter with the increased mechanical strain. The average fiber diameter of M0-laden tissue matrix was 0.27 ± 0.1 μm in the control group (0%), whereas the collagen fiber diameter was 0.22 ± 0.06 , 0.24 ± 0.1, and 0.22 ± 0.07 μm for 3%, 6%, and 12% mechanical strain groups, respectively.

However, the fiber diameters of all strain groups of M0-laden tissue matrices are in the same range as it is shown in the box plots of Figure 4C. The 25th percentile of fiber diameters in M0-laden tissue matrices falls within the range of 0.17 ± 0.01 μm for all strain groups. Also, the 75th percentile of fiber diameters in M0-laden tissue matrices falls within the range of 0.28 ± 0.02 μm for all strain groups.

On the other hand, the mechanical loading had a profound effect on structural features of the M1-laden tissue matrices. The SEM images (Fig. 4B) displayed a loose fiber configuration for 3% mechanical strained M1-laden tissue matrices compared with control, 6%, and 12% mechanical strained matrices. The fiber diameter analysis was conducted using SEM images (Fig. 4C).

On 3% mechanical loading, the diameter of collagen fibers in M1-laden tissue matrices decreased significantly ($p < 0.05$) compared with 0%, 6%, and 12% mechanical strained matrices. The average fiber diameters were

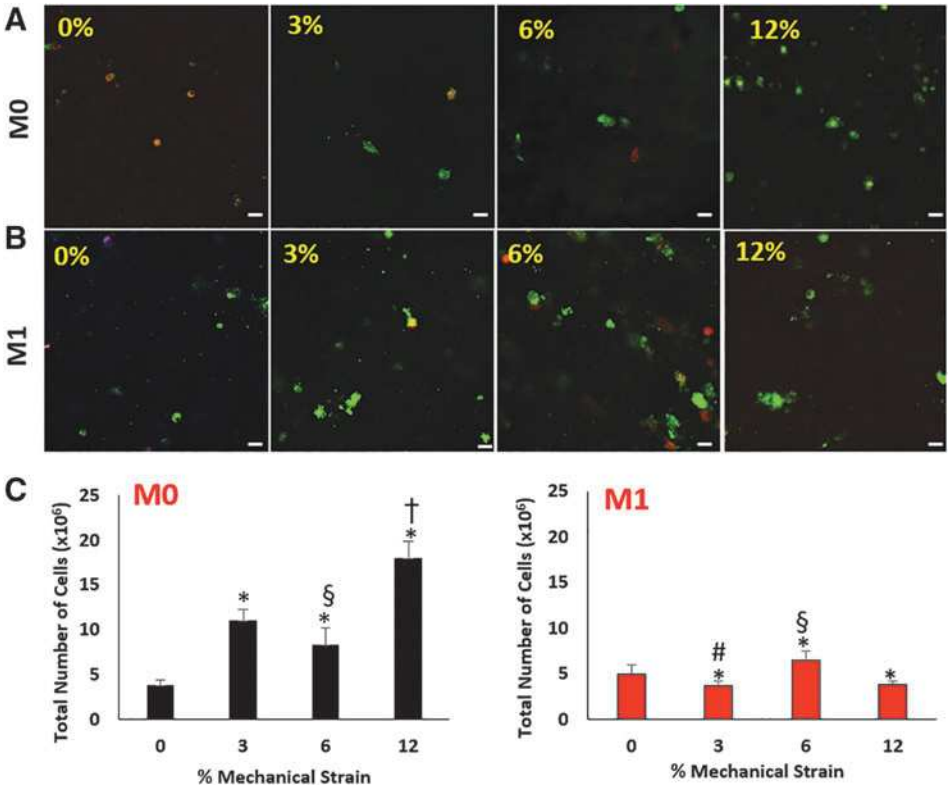

FIG. 3. **(A, B)** Double staining of live (*green*) and dead (*red*) M0 and M1 macrophages on mechanical loading, respectively. Scale bar represents 10 μm **(C)** The number of live M0 and M1 cells within the 3D tissue matrix following the mechanical loading. *Indicates a significant difference with respect to the 0% strain group (control). #Represents a significant difference between 3% and 6% mechanically strained groups, §represents a significant difference between 6% and 12% mechanically strained groups, and †represents a significant difference between 3% and 12% each with $p < 0.05$.

0.2 ± 0.07, 0.19 ± 0.08, and 0.21 ± 0.06 μm, for 0%, 6%, and 12% mechanical strained matrices, respectively, whereas the fiber diameter was 0.16 ± 0.06 μm for 3% mechanical strained matrices.

Similarly, the box plots of Figure 4C show that the interquartile range of fiber diameters in M1-laden tissue exposed to 3% mechanical strain is significantly lower than the control and 6% strain groups. There was a statistically significant change in M1-laden tissue matrix on 3% mechanical loading, and the collagen fibers were further assessed using histology slides. Masson's trichrome-stained collagen fibers in histology images provided tissue-scale information compared with micron-scale very zoomed SEM images.

The histology images (Fig. 4D) further confirmed the fact that when M1-laden collagen matrix is exposed to 3% mechanical strain, it has a loose fibrillary structure compared with the control and other mechanical loading groups. The data overall demonstrated that the effect of mechanical loading on 3D collagen matrices was cell-specific and most likely affected by the phenotypes of the macrophages.

The sub-phenotype specific mechano-responsiveness of macrophages

Before conducting an extensive gene expression analysis on M0 and M1 cells on mechanical loading, we studied whether the mechanical strain applied on macrophage-laden 3D matrix would be translated into a cellular response through assessing the c-Fos expression. c-Fos is an immediate early mechanoresponsive gene that is upregulated if any mechanical perturbation is exerted on the tissue.[48] Figure 5 demonstrates the changes in c-Fos expression, with the increased mechanical strain applied to M0- and M1-laden 3D tissue matrices.

Following a 7-day mechanical loading, for M0 macrophages, there was no statistical difference in c-Fos expression between 0% (control) and 3 and 6% mechanical strained groups. Yet, between the 3% and 6% mechanical strained groups, the c-Fos expression was significantly ($p < 0.005$) lower in 3% mechanically strained M0 macrophages compared with 6% of their strained counterparts.

The c-Fos expression of M0 cells only upregulated statistically significant ($p < 0.005$) for the 12% mechanically strained group with almost 15-fold compared with the control group (0%). For M1 macrophages, M1 c-Fos expression was significantly increased in all mechanically loaded M1 macrophages compared with the control group (0%).

The c-Fos expression upregulation was 2.7 ± 0.49-fold, 18.47 ± 0.65-fold, and 22.19 ± 0.4-fold for 3%, 6%, and 12% mechanically strained samples, respectively, compared with control groups. However, between the mechanically loaded M1 macrophages, the c-Fos expression was statistically significantly ($p < 0.005$) lower for 3% mechanically strained groups compared with 6% and 12% of their strained counterparts; there was no statistical difference between the 6% and 12% groups.

Overall, the c-Fos expression data (Fig. 5) demonstrated that mechanical loading applied to the 3D matrix translated into the macrophages within the 3D matrix but the mechano-responsiveness of macrophages was sub-phenotype specific. The M1 macrophages were more susceptible to mechanical loading compared with M0 macrophages. M1 macrophages

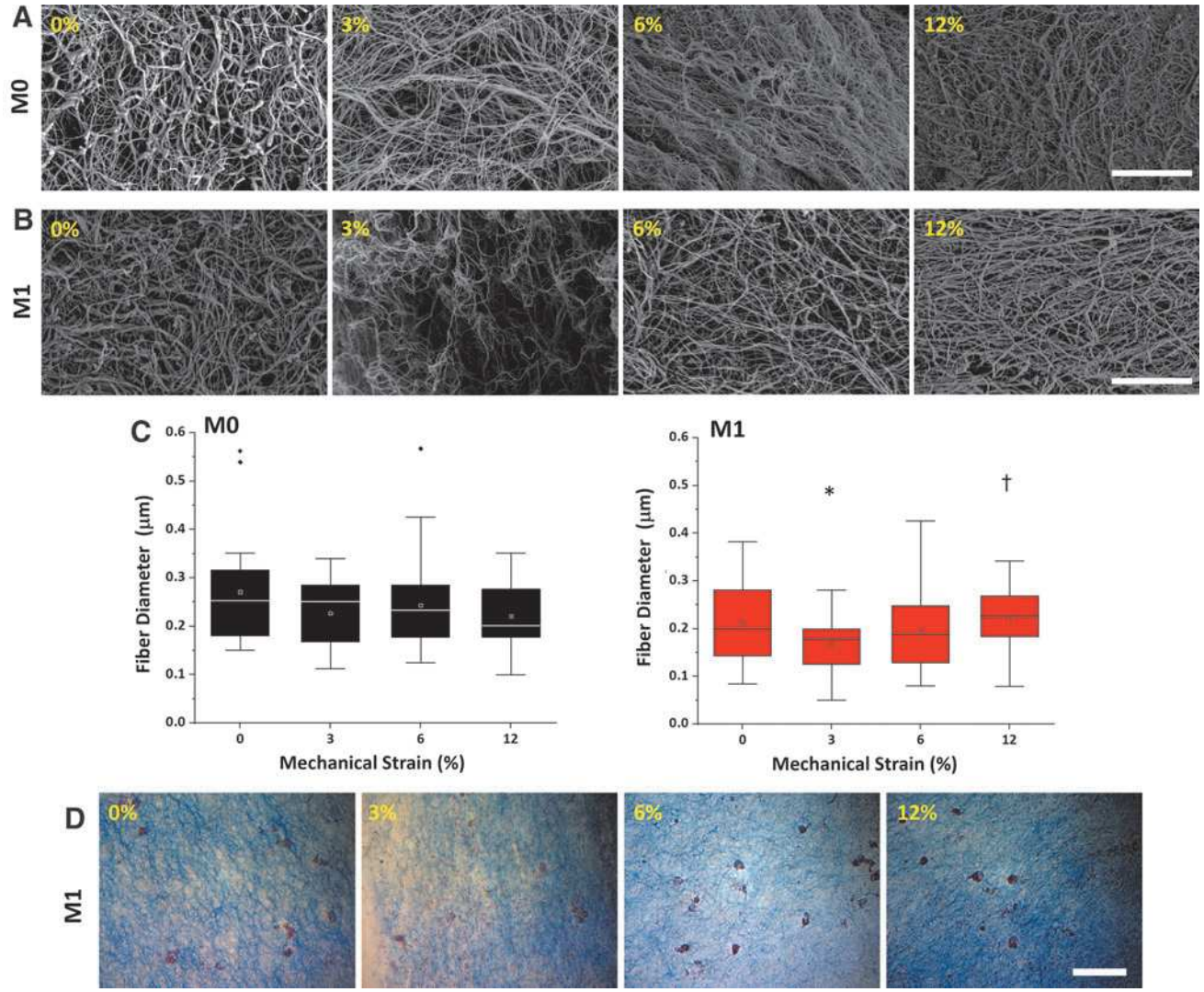

FIG. 4. **(A, B)** Representative SEM images of the M0-laden and M1-laden tissue matrices, respectively, on 0%, 3%, 6%, and 12% mechanically strained applications. Scale bar represents 10 μm. **(C)** Three fields of view from each sample were analyzed by ImageJ, and the *box plots* represent the changes in median fiber diameter of M0-laden and M1-laden tissue matrices on 0%, 3%, 6%, and 12% mechanical strains. The *black box* and *red box* show interquartile range (25–75%) of the fiber diameters in M0-laden matrices and M1-laden matrices, respectively. The small *square* inside the interquartile range shows the mean of each strain group. *Indicates a significant difference with respect to the 0% strain group (control). #Represent a significant difference between 3% and 6% mechanically strained groups, and †represents a significant difference between 3% and 12% each with $p < 0.05$. **(D)** Representative optical images of Masson's trichrome-stained M1-laden tissue matrix on mechanical loadings. The collagen fibers stained in *blue*, whereas the cell nucleus stained with *purple* color. The scale bar represents 5 μm. SEM, scanning electron microscopy.

effectively converted even relatively low (3%) mechanical strain to the early cellular response compared with naive macrophages.

To understand the possible reason for observing differences in mechano-responsiveness between M0 and M1 macrophages, the intracellular filamentous actin (F-actin) structures and intensity were assessed for M0 and M1 macrophages. When macrophages polarize from naive state (M0) to pro-inflammatory state (M1), the macrophage cytoskeletal deforms,[11,49] which further alters chromatin structure and thus modulates gene transcriptional activity.[50]

Considering the role of the cell cytoskeleton in mechanosensitivity of the mammalian cells, F-actin structure was studied through immunofluorescence imaging and comparing fluorescence intensity of the labeled F-actin between M0 and M1 macrophages. Figure 6 demonstrates the striking differences in the density and structure of actin filaments (F-actin) in M0 and M1 macrophages.

M0 macrophages within the 3D collagen matrices demonstrated elongated, flattened, and more spread-out morphology with lower intensity of brightness of staining, which shows lower F-actin content. Moreover, F-actin was not homogenously distributed, and some more intense staining appeared around the cell membrane. By contrast, in M1 macrophages, the intensity of brightness of F-actin was higher and F-actin appeared predominantly in highly dense deposits at the cell center and in a closely packed structure.

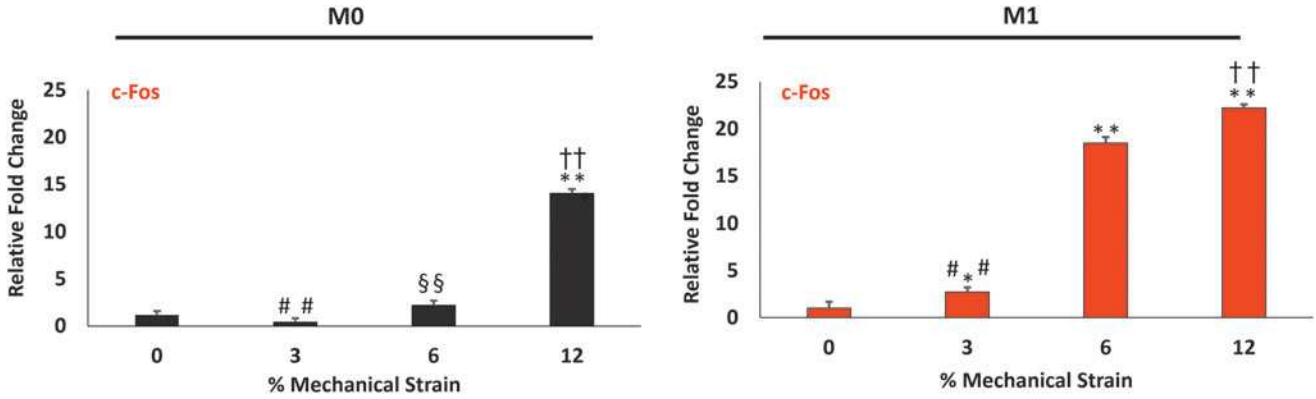

FIG. 5. Effect of various mechanically strained amplitudes on the expression of early mechano-responsive gene, c-Fos, for M0 and M1 residing within the 3D tissue matrix. *Indicate a significant difference with respect to the 0% strain group (control). #Represent a significant difference between 3% and 6% mechanically strained groups, §represent a significant difference between 6% and 12% mechanically strained groups, and †represent a significant difference between 3% and 12% strained groups, each with a 0.05 p-value. **shows that the statistical difference with respect to the 0% strain group (control) has a significance level of $p < 0.005$. ##shows that the statistical difference between the 3% and 6% mechanically strained group has a significance level of $p < 0.005$. ††shows that the statistical difference between the 3% and 12% mechanically strained group has a significance level of $p < 0.005$.

These qualitative observations were corroborated by the quantitative analysis of the cell morphology conducted through ImageJ. As demonstrated in Figure 6 data point graph, the average F-actin per unit area in M0 macrophages is 31.85 ± 18.46 whereas it is significantly higher in M1 macrophages (67.27 ± 23.6). Different levels of F-actin contents between M0 and M1 macrophages show various levels of mechano-sensitivity[51–53] between these two phenotypes.

The sub-phenotype specific changes in pro- and anti-inflammatory markers expression on mechanical loading

On confirmation on mechano-responsiveness of M0 and M1 within the 3D matrix, next, we have investigated whether various mechanical loading (3%, 6%, and 12%) applied to the 3D tissue matrix modulates the phenotypic changes in naive and pro-inflammatory macrophages differently. The changes in the relative expression of prominent pro-inflammatory and matrix degradation markers, along with anti-inflammatory markers were assessed using qRT-PCR following various mechanical loadings.

Figure 7 shows the relative gene expression of pro-inflammatory genes including TNF-α, IL-1β along with matrix degradation marker MMP3 for M0 and M1 macrophages within the 3D matrix experienced various mechanical loading (0, 3, 6, and 12% strains).

For M0 macrophages within the 3D matrix, the pro-inflammatory gene, TNF-α, was significantly ($p < 0.05$) upregulated with 12-fold change in 12% mechanically strained groups compared with the 0% strained group (control). There was a slight statistical increment in TNF-α expression from 3% strained groups to 6% groups, whereas there was no statistical difference between 3% and 6% mechanically strained groups compared with the control (0%).

For M1 macrophages, the TNF-α expression increased almost five-fold for 3% mechanically strained matrices compared with the control. However, the TNF-α expression was not statistically different for 6% strained groups compared with the control (0%). For supra-loading (12%), although there was a slight upregulation in TNF-α expression compared with the control, it was significantly lower than the 3% mechanically strained counterparts.

For IL-1β and MMP3 expression in M0 macrophages, the mechanical loading did not statistically significantly affect the relative fold changes of these genes' expression. There was no statistical difference between the IL-1β and MMP3 expression of all M0-laden mechanically loaded groups (3%, 6%, and 12%) and the control (0%) groups. For M1 macrophages, the pro-inflammatory gene expression trend was different than M0 macrophages.

For M1 macrophages, the 3% mechanical strain promoted the highest relative fold change in TNF-α, IL-1β, and MMP3 gene expression compared with the control and other mechanically loaded counterparts. For M1 macrophages, in the 3% mechanically strained groups, the TNF-α, IL-1β, and MMP3 expression upregulated statistically significantly with 4.8 ± 0.57-fold, 6.15 ± 0.74-fold, and 13.7 ± 0.51-fold, respectively, compared with the control group (0%).

For the 6% mechanically strained M1 macrophages, there was no statistical difference in IL-1β expression compared with the control, whereas there was a slight upregulation in TNF-α (1.5 ± 0.59-fold) and MMP3 expression (6.28 ± 0.76-fold) compared with control groups. For the 12% mechanically strained M1 macrophages, compared with control groups, only TNF-α and IL-1β were statistically different than the control group.

The changes in anti-inflammatory gene expression on various mechanical loading were also studied for M0 and M1 macrophages. Figure 8 shows the relative gene expression of anti-inflammatory genes, including CD163, CCL18, and IL-10, for M0 and M1 macrophages within the 3D matrix experienced various mechanical loading (0%, 3%, 6%, and 12% strains).

As shown in Figure 8, for naive macrophages (M0) encapsulated in 3D collagen matrices, the expression of CD163, CCL18, and IL-10 anti-inflammatory genes upregulated statistically significantly when the M0 macrophages

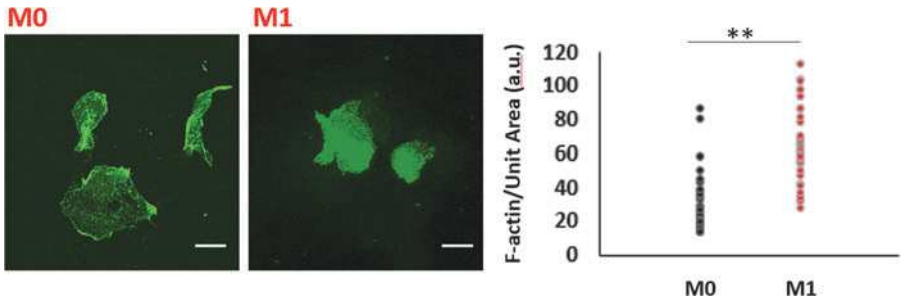

FIG. 6. Representative confocal image of the M0 and M1 macrophages stained with Alexa Fluor® 488 phalloidin. Scale bar represents 10 μm. Individual datapoint plot shows F-actin per unit area quantification of M0 and M1 macrophages. **Indicate a significant difference between M0 and M1 macrophages, with a $p < 0.005$.

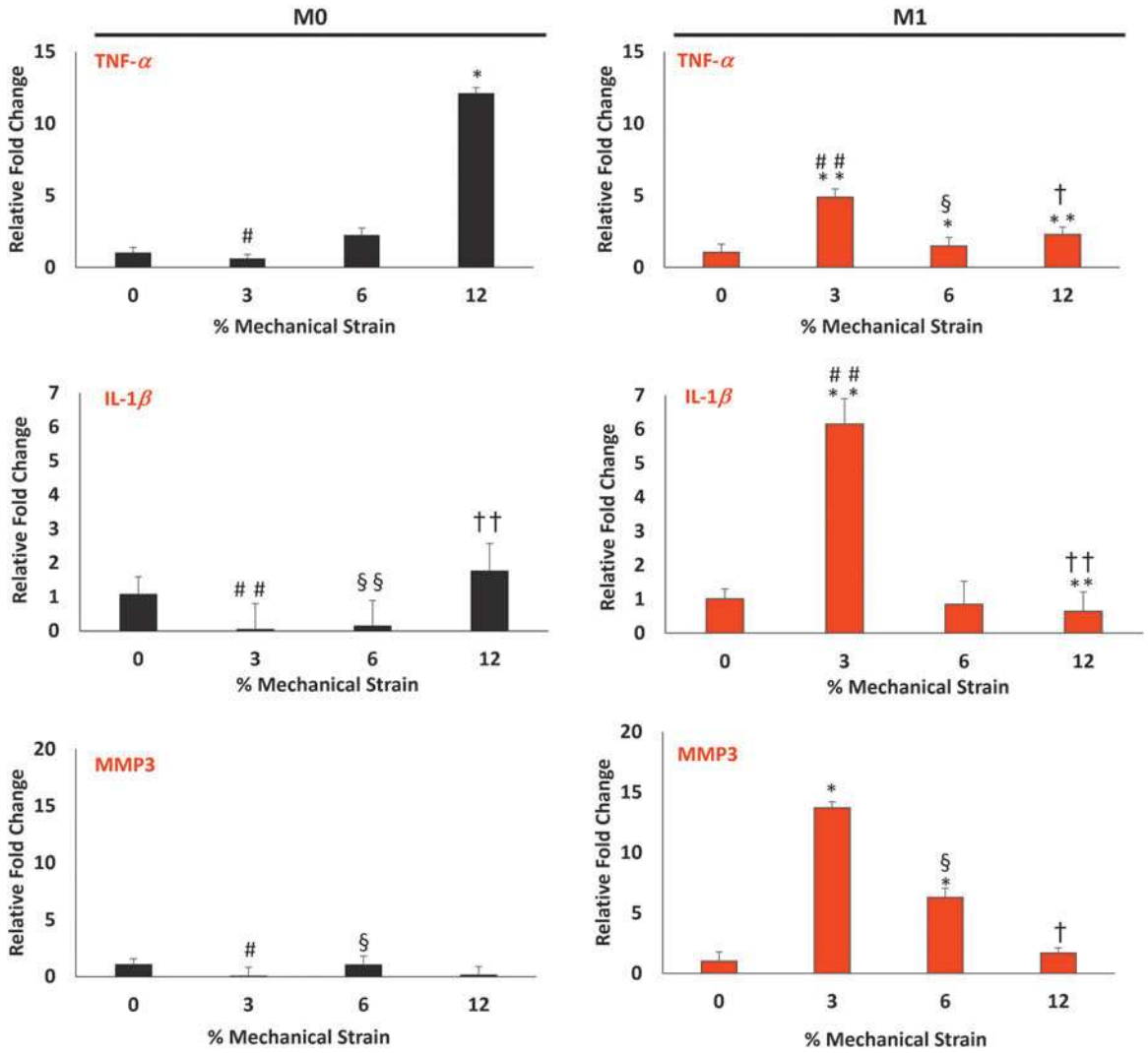

FIG. 7. Effect of various mechanical strain amplitudes on the gene expression of pro-inflammatory and matrix degradation markers in both M0- and M1-laden 3D tissue matrix. *Indicate a significant difference with respect to the 0% strain group (control). #Represent a significant difference between 3% and 6% mechanical strain groups, §represent a significant difference between 6% and 12% mechanical strain groups, and †represent a significant difference between 3% and 12% strain groups, each with a 0.05 p-value. **shows that the statistical difference with respect to the 0% strain group (control) has a significance level of $p < 0.005$. ##shows that the statistical difference between the 3% and 6% mechanical strain group has a significance level of $p < 0.005$. §§shows that the statistical difference between the 6% and 12% mechanical strain group has a significance level of $p < 0.005$. ††shows that the statistical difference between the 3% and 12% mechanical strain group has a significance level of $p < 0.005$.

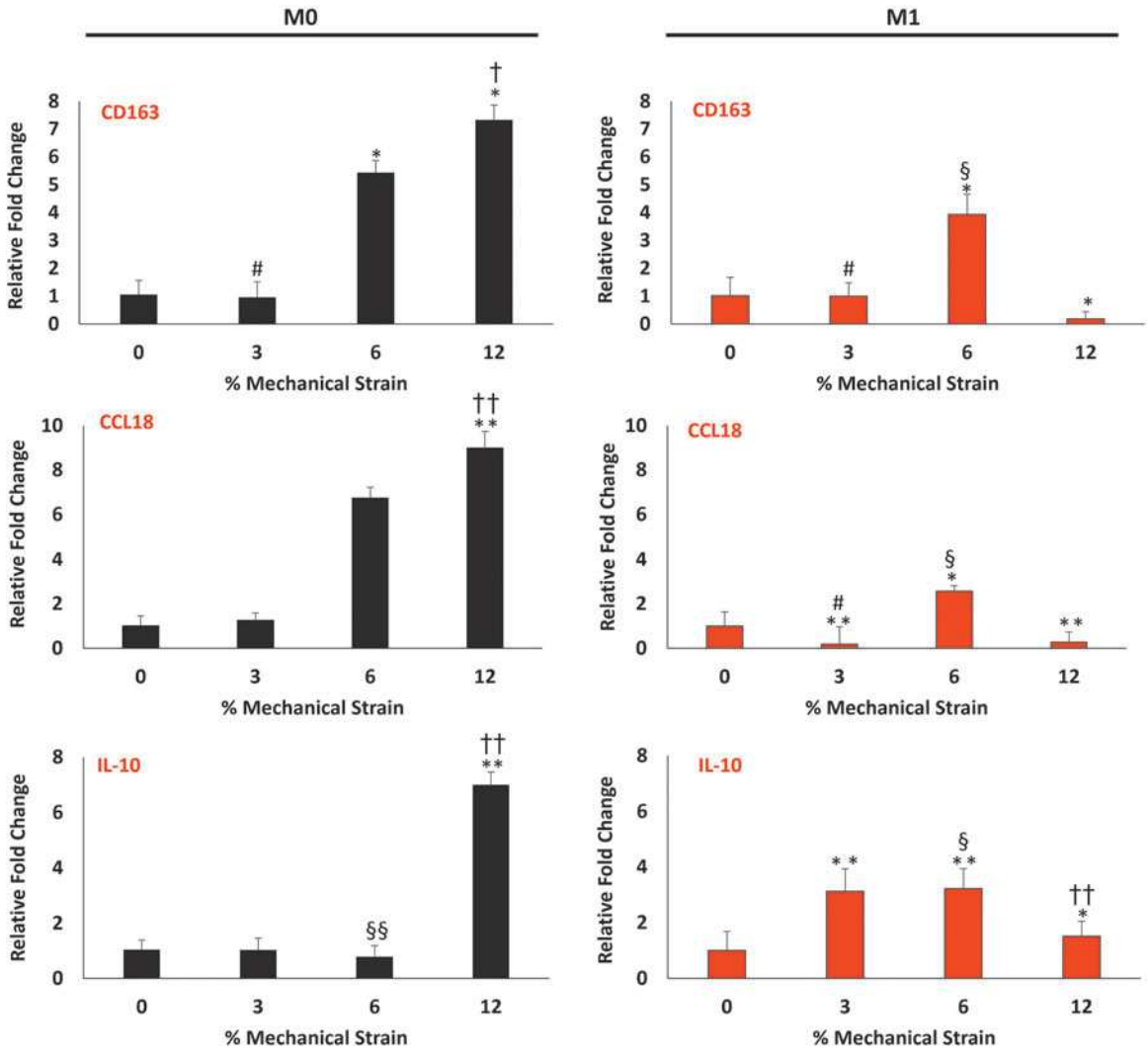

FIG. 8. Effect of various mechanical strain amplitudes on the gene expression of anti-inflammatory markers in both M0- and M1-laden 3D tissue matrix. *Indicate a significant difference with respect to the 0% strain group (control). #Represent a significant difference between the 3% and 6% mechanical strain groups, §represent a significant difference between the 6% and 12% mechanical strain groups, and †represent a significant difference between the 3% and 12% strain groups, each with a 0.05 p-value. **shows that the statistical difference with respect to the 0% strain group (control) has a significance level of $p<0.005$. §§shows that the statistical difference between the 6% and 12% mechanical strain group has a significance level of $p<0.005$. ††shows that the statistical difference between the 3% and 12% mechanical strain group has a significance level of $p=0.005$.

were exposed to hyper-mechanical strain (12%). The relative fold change in mRNA expression of CD163, CCL18, and IL-10 increased almost 7.33 ± 0.53-fold, 8.97 ± 0.76-fold, and 7.0 ± 0.46-fold, respectively, at 12% mechanically strained matrices compared with the control group (0%).

The anti-inflammatory genes expressed lowest at the 3% mechanically strained groups, with no statistical difference between control groups and only increased statistically significant level ($p<0.05$) for CD163 expression at 6% mechanically strained matrices.

For M1 macrophages, the anti-inflammatory genes expressed the highest 6% mechanically strained matrices compared with 0% (control), 3%, and 12% mechanically strained counterparts. The CD163, CCL18, and IL-10 expression upregulated almost 3.93 ± 0.73-fold, 2.57 ± 0.23-fold, and 3.22 ± 0.71-fold, respectively, at 6% mechanically strained matrices compared with the control group (0%).

Beyond the 6% mechanical strain, the anti-inflammatory gene expression decreased statistically significantly (for CCL18 $p<0.005$ and for CD163 and IL-10 $p<0.05$). Overall, the data indicated that M1 macrophages exposed to 6% mechanical strain demonstrated the highest phenotypic shift toward anti-inflammatory phenotypes compared with the counterparts exposed to 3% and 12% mechanical strain.

Figure 9 gives the heatmap visually demonstrating how pro- and anti-inflammatory gene expression changes as a function of mechanical strain amplitudes for M0 and M1 macrophages. The color gradients were a substitute for numerical variations of z-scores associated with

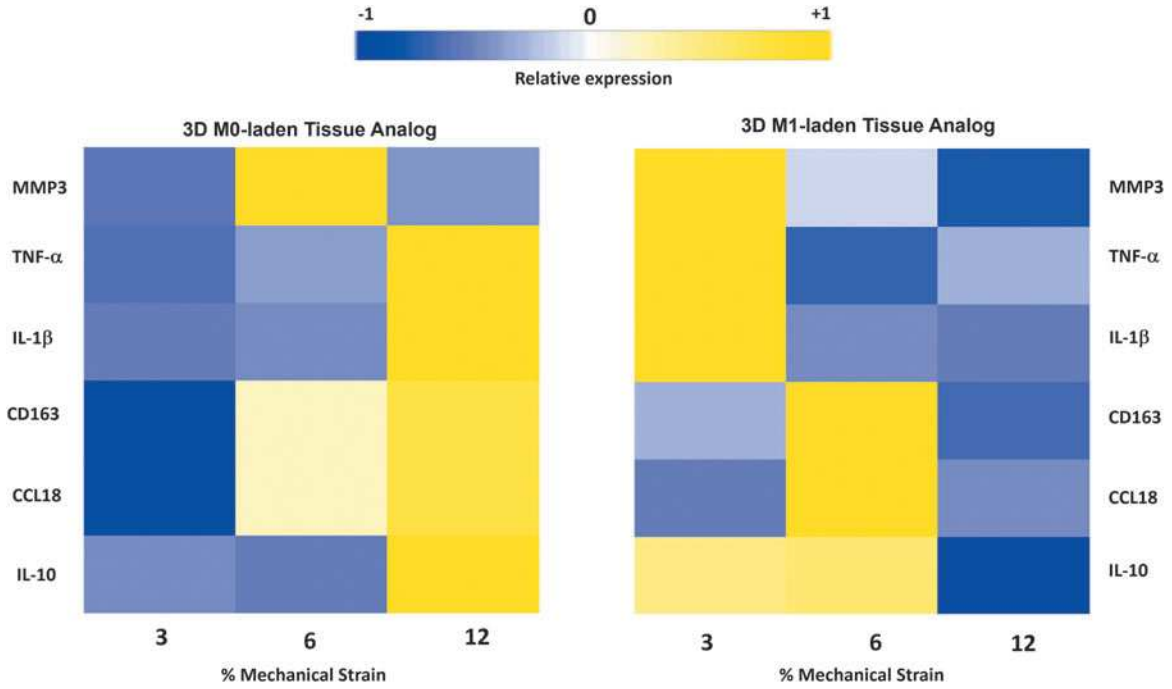

FIG. 9. The heatmap of pro- and anti-inflammatory gene expression changes as a function of mechanical strain values. The *yellow* indicates gene upregulation, whereas the *blue* shows gene downregulation.

relative fold change. The gradual color change from blue (negative z-score) to yellow (positive z-score) indicates gene upregulation.

Overall, the gene expression data suggested that when the M1-laden tissue was exposed to 3% mechanical strain M1 macrophages expressed dominantly pro-inflammatory markers and tended to preserve its pro-inflammatory phenotype. When the M1-laden tissue was exposed to 6% mechanical strain, the anti-inflammatory markers expressed significantly, which promoted phenotypic shifts of M1 macrophages from pro-inflammatory to pro-healing lineage. For M0 macrophages, the phenotypic shift toward pro- and anti-inflammatory lineages required supra-mechanical loading (12% mechanical strain). Specifically, with 12% mechanical strain, M0 cells tended to polarize into anti-inflammatory lineage.

Discussion

The innate immune cells, specifically macrophages, play a critical role in MSK tissue healing and hemostasis.[54] In fact, the macrophage-depleted animal studies demonstrated that bone, muscle,[55,56] and tendon[57,58] tissues do not heal without the direct involvement of macrophages. Considering the frequency of MSK injuries and the fact that the mechanotherapy exercises are routinely employed during MSK tissue injuries,[25,59,60] it is important to understand how mechanical loading experienced by MSK tissues during the mechanotherapy exercises affects the phenotypic changes in naive (M0) and pro-inflammatory (M1) macrophages.

In other words, there is a need for understanding whether mechanical loadings applied during mechanotherapy exercises translate into immunomodulation (mechano-immunomodulation) and whether the effect is macrophage sub-phenotype specific. To this end, we first elucidated the different mechano-responsiveness of macrophage sub-phenotypes to the same mechanical loading condition. We then studied the effects of various mechanical strain amplitudes on each macrophage sub-phenotype.

Before synthesizing the macrophage-laden 3D collagen matrix and conducting extensive molecular studies on macrophages, the phenotypic differentiation was confirmed for both M0 and M1 macrophages through immunohistochemistry (Fig. 2). The protein staining confirmed that naive macrophages (M0) were differentiated from blood-derived human monocyte, whereas the pro-inflammatory macrophages (M1) were polarized successfully from naive macrophages. On phenotypic confirmation, the M0 and M1 macrophages were encapsulated within the 3D collagen matrix and exposed to various mechanical loading amplitudes (0%, 3%, 6%, and 12%) experienced during mechanotherapy exercises.[61,62]

First, the viability of macrophages was assessed following 7 days of various mechanical loading of the 3D collagen matrix. The qualitative and quantitative cell viability data (Fig. 3) demonstrated that even the supra-mechanical loading (12%) did not kill the M0 and M1 macrophages within the 3D collagen matrices. These data may contradict with the literature, demonstrating that high mechanical strain exposure creates cell membrane damage and blebbing that leads to cell death.[63–65]

The data discrepancy can be attributed to the differences in how macrophages were exposed to the mechanical loading. In the current study, M0 and M1 macrophages were exposed to various mechanical strains while being encapsulated within a 3D collagen matrix. Yet, the majority studies in this field investigated the response of

macrophages cultured on two-dimensional (2D) surfaces (e.g., elastic membranes or petri dishes), where macrophages were not surrounded with the 3D matrix during the mechanical loading.

It is important to acknowledge that subjecting 3D collagen matrices to loading introduces macrophages to multifaceted mechanical forces. The residing cells within the mechanically loaded 3D collagen matrix are exposed to forces in many directions that create compression, tension, and shear forces on cells.[66] The collagen fibrous structures surrounding macrophages have an impact on macrophage differentiation through influencing the reorganization of the cytoskeleton and the downstream signaling pathways that regulate macrophage phenotype.[67]

In addition, the interstitial fluid within this context establishes a dynamic microenvironment that significantly impacts the macrophage phenotype through the transport of soluble factors[68] and contributes to flow-induced macrophage polarization.[69] In addition, in 2D culture, the strain applied to cells is limited by the stiffness of the underlying surface, potentially influencing the cellular response to mechanical stimuli.

Once the viability of encapsulated macrophages within 3D collagen matrices was established even under the supra-mechanical loading (12%) condition, then the structural changes within the 3D collagen matrix were assessed using SEM and histology data (Fig. 4). The SEM images, the quantitative fiber diameter analysis, and histology images all demonstrated that when the M1-laden collagen matrix was loaded with 3% mechanical strain, the collagen fiber structure was loose and fiber diameter decreased significantly ($p < 0.05$) when compared with 0%, 6%, and 12% mechanically strained groups.

On the other hand, no statistical structural changes were observed in the M0-laden collagen matrix exposed to 0%, 3%, 6%, and 12% mechanical strains. The overall data demonstrated that the remodeling potential of ECM circulating around the macrophages depended on both phenotype of encapsulated macrophages and mechanical loading amplitude applied to the matrices.

The increased proteolytic activity of M1 macrophages and secretion of expressions of matrix metalloproteins (MMPs) under 3% mechanical strain could be the reason for the decreased collagen fiber diameter and loose collagen structures. Thus, we have conducted a gene expression analysis to study the mechanomics of naive and M1 macrophages, their mechano-responsiveness, and phenotypic commitments using gene expression analysis.

To study how mechanical loading modulates the naive and M1 macrophages behavior (mechanomics of macrophages), first, their mechano-responsiveness was evaluated through measuring the changes in c-Fos expression with the various mechanical loading. In this study, the c-Fos expression was used as a measure of mechano-responsiveness of macrophages on mechanical loading because c-Fos is the commonly utilized marker of mechano-responsiveness.[70]

The *in vitro* and *in vivo* studies demonstrated that the c-Fos and c-Jun transcription factors in the axis of AP-1 pathway have been upregulated and used as a mechano-responsiveness marker for various cell types, including megakaryocytes,[70] osteocytes,[71] osteoblasts,[72] and fibroblasts,[40] on mechanical loading.

The results presented in Figure 5 demonstrate that M0 and M1 macrophages responded differently to the mechanical strains as evidenced by mechanical induction of the early response gene of c-Fos. The degree of this mechano-responsiveness of M0 and M1 cells appeared to depend on the differentiation state of the macrophages and the magnitude of the mechanical loading.

The M1 macrophages demonstrated a more robust mechano-response than M0 macrophages with upregulated c-Fos expression with the increased mechanical strain amplitudes (Fig. 5). For M1 macrophages, 3% mechanical strain was enough to induce an early mechanical response with a statistically significant ($p < 0.05$) increase in c-Fos expression compared with the control (0% mechanical strain).

For M0 macrophages, the M0-laden collagen matrices needed to be loaded with supra-mechanical loading (12%) to have a statistically significant ($p < 0.05$) upregulation in c-Fos expression. This may indicate that M1 macrophages are more sensitive to mechanical cues than naive (M0) macrophage cells.

The different mechano-responsiveness between M0 and M1 can be attributed to the variations in cytoskeletal tensegrity between two cells. The cytoskeletal components play a crucial role in determining the mechanical properties of cells[45] and defining the cellular response to mechanical stimuli through tuning cell stiffness, deformability, and contractility. When cells residing within a tissue experience mechanical force, the cytoskeleton, mainly filamentous actin (F-actin), serves as the primary conduit to transmit mechanical signals to the cell nucleus, triggering various responses, including alterations in gene expression and cell behavior.[73,74]

In the case of macrophages, the cytoskeletal content and distribution significantly influence their capacity for polarization under mechanical cues. For instance, Tu et al.[75] demonstrated that uniaxial stretch induced alterations in macrophage morphology and gene expression profile. These findings underscore the fundamental role of the cytoskeleton in governing cell mechanics and facilitating adaptive responses to mechanical stimuli.

Thus, in this study, the F-actin structure of M0 and M1 cells was visualized and analyzed. The data (Fig. 6) demonstrated that F-actin density was higher in M1 macrophages, which might cause M1 macrophages to sense and respond to even smaller mechanical perturbations (3%) effectively than M0 macrophages. Several prominent studies also arrived at the same conclusion that different levels of F-actin contents between M0 and M1 macrophages lead to different levels of mechano-sensitivity between two phenotypes.[51–53]

Once we have established the difference in mechano-responsiveness of naive and pro-inflammatory macrophages, the mechanome of macrophages was then mapped out. The mechanome dataset was related to the macrophage polarization by the cross-referencing applied mechanical strain and the subsequent up- and downregulation of pro- and anti-inflammatory gene expression.

Figures 7 and 8 demonstrated the changes in expression of pro- and anti-inflammatory markers for M0 and M1 macrophages within 3D collagen matrices under 0%, 3%, 6%, and 12% mechanical strain loading. The pro-inflammatory gene expression data (Fig. 7) suggested that M0 macrophages expressed prominent pro-inflammatory gene

such as TNF-α, only when they are exposed to the supra-mechanical loading condition (12% mechanical strain).

The mechanical loading did not significantly ($p < 0.05$) affect the TNF-α, IL-1β genes expression. For M1 macrophages, the highest upregulation of inflammatory genes (TNF-α, IL-1β, and MMP3) was observed in samples that were exposed to 3% mechanical strain. These data suggested that proteolytic activities of M1 macrophages increased with the increased MMP3 expression when M1 macrophages within the tissue were exposed to 3% mechanical strain.

These data also agreed with the structural analysis of M1-laden 3D collagen matrices on mechanical loading (Fig. 4), which demonstrated that there was a significant reduction in collagen fiber diameter and loose ECM around the cells only when the M1-laden collagen matrix was exposed to 3% mechanical strain. The expression of pro-inflammatory genes, TNF-α, IL-1β, and MMP3, leveled down with the increased mechanical strain amplitudes (6% and 12%) for M1 macrophages.

The anti-inflammatory gene expression data (Fig. 8) suggested that CD163, CCL18, and IL-10 expression increased significantly for M1 macrophages on 6% mechanical strain application. All in all, the pro- and anti-inflammatory gene expression data (Figs. 7 and 8) of M1 and M0 macrophages demonstrated the immunomodulation potential of mechanical loading experienced by the tissues within which M0 and M1 macrophages resided.

The gene expression data suggested that when the M1-laden tissue was exposed to 3% mechanical strain, M1 macrophages expressed dominantly pro-inflammatory markers and tended to preserve its pro-inflammatory phenotype. When the M1-laden tissue was exposed to 6% mechanical strain, the anti-inflammatory markers expressed significantly, which promoted phenotypic shifts of M1 macrophages from pro-inflammatory to pro-healing lineage.

For M0 macrophages, the phenotypic shift toward pro- and anti-inflammatory lineages required supra-mechanical loading (12% mechanical strain). Specifically, with 12% mechanical strain, M0 cells tended to polarize into anti-inflammatory lineage.

During mechanotherapy, the macrophages are exposed to various mechanical strains, which is still unclear as to how it influences macrophage polarization. Though there is a long way for clinical implications, the current study may elucidate new and informed directions for modulating the macrophage inflammatory response using mechanotherapy toward MSK tissue healing.

By utilizing biomimetic approaches, including macrophage-laden 3D matrices and physiologically relevant mechanical loading amplitudes, a deeper understanding of mechano-responsiveness of macrophages and its consequences in polarization was gained. Harnessing sub-phenotype specific macrophage mechano-responsiveness for mechanotherapy may improve the mechanotherapy application outcome in MSK tissue regeneration.

Acknowledgment

The authors thank the University of Toledo, Center for Materials and Sensor Characterization, for their access to the scanning electron microscope assistance.

Authors' Contributions

E.Y.-A., P.B., and D.J. conceived and planned the experiments. P.B., D.J., and A.T. carried out the experiments. P.B., D.J., and E.Y.-A. analyzed and interpreted the data. A.R. and R.G.-M. contributed to confocal image acquisition. P.B. contributed to image data analysis. E.Y.-A. and P.B. wrote the main article text. All authors reviewed and agreed to the final version of the article.

Disclosure Statement

No competing financial interests exist.

Funding Information

This study is supported by the National Science Foundation under Grant 2213958 (E.Y.-A.) and by the National Institute of Health under Grant R01GM136826 (R.G.-M.).

References

1. Wu F, Nerlich M, Docheva D. Tendon injuries: Basic science and new repair proposals. EFORT Open Rev 2017;2(7):332–342.
2. Lee CH, Lee FY, Tarafder S, et al. Harnessing endogenous stem/progenitor cells for tendon regeneration. J Clin Invest 2015;125(7):2690–2701.
3. Subramanian G, Stasuk A, Elsaadany M, et al. Effect of uniaxial tensile cyclic loading regimes on matrix organization and tenogenic differentiation of adipose-derived stem cells encapsulated within 3D collagen scaffolds. Stem Cells Int 2017;2017:6072406.
4. Dean BJF, Dakin SG, Millar NL, et al. Review: Emerging concepts in the pathogenesis of tendinopathy. Surgeon 2017;15(6):349–354.
5. Millar NL, Dean BJ, Dakin SG. Inflammation and the continuum model: time to acknowledge the molecular era of tendinopathy. Br J Sport Med 2016;50(23):1486.
6. Spiller KL, Freytes DO, Vunjak-Novakovic G. Macrophages modulate engineered human tissues for enhanced vascularization and healing. Ann Biomed Eng 2015;43(3):616–627.
7. Brown BN, Ratner BD, Goodman SB, et al. Macrophage polarization: An opportunity for improved outcomes in and regenerative medicine. Biomaterials 2012;33(15):3792–3802; doi: 10.1016/j.biomaterials.2012.02.034
8. Dumont CM, Park J, Shea LD. Controlled release strategies for modulating immune responses to promote tissue regeneration. J Control Release 2015;219:155–166; doi: 10.1016/j.jconrel.2015.08.014
9. Kjaer M, Bayer ML, Eliasson P, et al. What is the impact of inflammation on the critical interplay between mechanical signaling and biochemical changes in tendon matrix? J Appl Physiol 2013;115(6):879–883; doi: 10.1152/japplphysiol.00120.2013
10. Porcheray F, Viaud S, Rimaniol AC, et al. Macrophage activation switching: An asset for the resolution of inflammation. Clin Exp Immunol 2005;142(3):481–489.
11. McWhorter FY, Wang T, Nguyen P, et al. Modulation of macrophage phenotype by cell shape. Proc Natl Acad Sci U S A 2013;110(43):17253–17258; doi: 10.1073/pnas.1308887110
12. Hortensius RA, Ebens JH, Dewey MJ, et al. Incorporation of the amniotic membrane as an immunomodulatory design element in collagen scaffolds for tendon repair. ACS Biomater Sci Eng 2018;4(12):4367–4377.

13. Snedeker JG, Foolen J. Tendon injury and repair: A perspective on the basic mechanisms of tendon disease and future clinical therapy. Acta Biomater 2017;63:18–36; doi: 10.1016/j.actbio.2017.08.032
14. Gu Q, Yang H, Shi Q. Macrophages and bone inflammation. J Orthop Translat 2017;10:86–93.
15. Zhang YJ, Chen X, Li G, et al. Concise review: Stem cell fate guided by bioactive molecules for tendon regeneration. Stem Cell Transl Med 2018;7(5):404–414.
16. Cho JY. Immunomodulatory effect of nonsteroidal anti-inflammatory drugs (NSAIDs) at the clinically available doses. Arch Pharm Res 2007;30(1):64–74; doi: 10.1007/BF02977780
17. Hettinger Z, Harrison D, Butterfield T, et al. Single cell transcriptomics identifies immunomodulation in fibro-adipose progenitor cells and changes to macrophage dynamics following mechanotherapy in aged rats recovering from disuse muscle atrophy. FASEB J 2021;35(S1):02919; doi: https://doi.org/10.1096/fasebj.2021.35.S1.02919
18. Su B, O'Connor JP. NSAID therapy effects on healing of bone, tendon, and the enthesis. J Appl Physiol 2013;115(6):892–899; doi: 10.1152/japplphysiol.00053.2013
19. Fowler C. Do nonsteroidal anti-inflammatory drugs impair tissue healing? JAAPA 2018;31(8):1–5; doi: 10.1097/01.JAA.0000541488.41149.95
20. Wu AC, Raggatt LJ, Alexander KA, et al. Unraveling macrophage contributions to bone repair. Bonekey Rep 2013;2:373.
21. Ferry ST, Afshari HM, Lee JA, et al. Effect of prostaglandin E2 injection on the structural properties of the rat patellar tendon. Sports Med Arthrosc Rehabil Ther Technol 2012;4(1):2; doi: 10.1186/1758-2555-4-2
22. Lu Y, Li Y, Li FL, et al. Do different cyclooxygenase inhibitors impair rotator cuff healing in a rabbit model? Chin Med J (Engl) 2015;128(17):2354–2359; doi: 10.4103/0366-6999.163379
23. Soreide E, Granan LP, Hjorthaug GA, et al. The effect of limited perioperative nonsteroidal anti-inflammatory drugs on patients undergoing anterior cruciate ligament reconstruction. Am J Sports Med 2016;44(12):3111–3118; doi: 10.1177/0363546516657539
24. Sauerschnig M, Stolberg-Stolberg J, Schmidt C, et al. Effect of COX-2 inhibition on tendon-to-bone healing and PGE2 concentration after anterior cruciate ligament reconstruction. Eur J Med Res 2018;23(1):1; doi: 10.1186/s40001-017-0297-2
25. Khan KM, Scott A. Mechanotherapy: How physical therapists' prescription of exercise promotes tissue repair. Br J Sports Med 2009;43(4):247–251.
26. Trumbull A, Subramanian G, Yildirim-Ayan E. Mechanoresponsive musculoskeletal tissue differentiation of adipose-derived stem cells. Biomed Eng Online 2016;15:43; doi: 10.1186/s12938-016-0150-9
27. Leigh DR, Abreu EL, Derwin KA. Changes in gene expression of individual matrix metalloproteinases differ in response to mechanical unloading of tendon fascicles in explant culture. J Orthop Res 2008;26(10):1306–1312; doi: 10.1002/jor.20650
28. Abreu EL, Leigh D, Derwin KA. Effect of altered mechanical load conditions on the structure and function of cultured tendon fascicles. J Orthop Res 2008;26(3):364–373; doi: 10.1002/jor.20520
29. Khayyeri H, Blomgran P, Hammerman M, et al. Achilles tendon compositional and structural properties are altered after unloading by botox. Sci Rep 2017;7(1):13067; doi: 10.1038/s41598-017-13107-7
30. Mutsuzaki H, Nakajima H, Wadano Y, et al. Influence of mechanical unloading on histological changes of the patellar tendon insertion in rabbits. Knee 2015;22(6):469–474; doi: 10.1016/j.knee.2015.03.004
31. Killian ML, Cavinatto L, Shah SA, et al. The effects of chronic unloading and gap formation on tendon-to-bone healing in a rat model of massive rotator cuff tears. J Orthop Res 2014;32(3):439–447; doi: 10.1002/jor.22519
32. Killian ML, Lim CT, Thomopoulos S, et al. The effect of unloading on gene expression of healthy and injured rotator cuffs. J Orthop Res 2013;31(8):1240–1248; doi: 10.1002/jor.22345
33. Heinemeier KM, Olesen JL, Haddad F, et al. Effect of unloading followed by reloading on expression of collagen and related growth factors in rat tendon and muscle. J Appl Physiol 2009;106(1):178–186; doi: 10.1152/japplphysiol.91092.2008
34. Chen K, Hu X, Blemker SS, et al. Multiscale computational model of Achilles tendon wound healing: Untangling the effects of repair and loading. PLoS Comput Biol 2018;14(12):e1006652; doi: 10.1371/journal.pcbi.1006652
35. Kinugasa R, Yamamura N, Sinha S, et al. Influence of intramuscular fiber orientation on the Achilles tendon curvature using three-dimensional finite element modeling of contracting skeletal muscle. J Biomech 2016;49(14):3592–3595; doi: 10.1016/j.jbiomech.2016.09.014
36. Bayer ML, Schjerling P, Herchenhan A, et al. Release of tensile strain on engineered human tendon tissue disturbs cell adhesions, changes matrix architecture, and induces an inflammatory phenotype. PLoS One 2014;9(1):e86078; doi: 10.1371/journal.pone.0086078
37. Yotsumoto T, Miyamoto W, Uchio Y. Novel approach to repair of acute achilles tendon rupture: Early recovery without postoperative fixation or orthosis. Am J Sports Med 2010;38(2):287–292; doi: 10.1177/0363546509351557
38. Matsumoto T, Delafontaine P, Schnetzer KJ, et al. Effect of uniaxial, cyclic stretch on the morphology of monocytes/macrophages in culture. J Biomech Eng 1996;118(3):420–422.
39. Roebke E, Jacho D, Eby O, et al. Injectable cell-laden nanofibrous matrix for treating annulus fibrosus defects in porcine model: An organ culture study. Life 2022;12(11):1866.
40. Jacho D, Rabino A, Garcia-Mata R, et al. Mechanoresponsive regulation of fibroblast-to-myofibroblast transition in three-dimensional tissue analogues: Mechanical strain amplitude dependency of fibrosis. Sci Rep 2022;12(1):16832.
41. Bayrak E, Yilgor Huri P. Engineering musculoskeletal tissue interfaces. Front Mater 2018;5:24.
42. Elsaadany M, Winters K, Adams S, et al. Equiaxial strain modulates adipose-derived stem cell differentiation within 3D biphasic scaffolds towards annulus fibrosus. Sci Rep 2017;7(1):12868; doi: 10.1038/s41598-017-13240-3
43. Elsaadany M, Harris M, Yildirim-Ayan E. Design and validation of equiaxial mechanical strain platform, EQUicycler, for 3D tissue engineered constructs. Biomed Res Int 2017;2017:3609703; doi: 10.1155/2017/3609703
44. Kanan M, Eby O, Kelkar A, et al. Electrical stimulation-mediated tissue healing in porcine intervertebral disc under mechanically dynamic organ culture conditions. Spine (Phila Pa 1976) 2022;47(10):764–772; doi: 10.1097/BRS.0000000000004331
45. McCullen SD, Haslauer CM, Loboa EG. Musculoskeletal mechanobiology: Interpretation by external force and engineered substratum. J Biomech 2010;43(1):119–127; doi: https://doi.org/10.1016/j.jbiomech.2009.09.017

46. Thapa B, Lee K. Metabolic influence on macrophage polarization and pathogenesis. BMB Rep 2019;52(6):360.
47. Li W, Katz BP, Spinola SM. Haemophilus ducreyi-induced interleukin-10 promotes a mixed M1 and M2 activation program in human macrophages. Infect Immun 2012;80(12): 4426–4434.
48. Curtis KJ, Coughlin TR, Varsanik MA, et al. Shear stress in bone marrow has a dose dependent effect on cFos gene expression in in situ culture. Cell Mol Bioeng 2019;12(6): 559–568.
49. Wosik J, Chen W, Qin K, et al. Magnetic field changes macrophage phenotype. Biophys J 2018;114(8):2001–2013; doi: https://doi.org/10.1016/j.bpj.2018.03.002
50. Kirby TJ, Lammerding J. Emerging views of the nucleus as a cellular mechanosensor. Nat Cell Biol 2018;20(4):373–381.
51. Gong X, Fan Y, Zhang Y, et al. Inserted rest period resensitizes MC3T3-E1 cells to fluid shear stress in a time-dependent manner via F-actin-regulated mechanosensitive channel (s). Biosci Biotechnol Biochem 2014;78(4):565–573.
52. Ronzier E, Rotty JD. The actin cytoskeleton regulates macrophage activation and inflammation. Biophys J 2021; 120(3):281a.
53. Ronzier E, Laurenson AJ, Manickam R, et al. The actin cytoskeleton responds to inflammatory cues and alters macrophage activation. Cells 2022;11(11):1806.
54. Jiang S, Lyu C, Zhao P, et al. Cryoprotectant enables structural control of porous scaffolds for exploration of cellular mechano-responsiveness in 3D. 2019;10(1):1–14.
55. Liu X, Liu Y, Zhao L, et al. Macrophage depletion impairs skeletal muscle regeneration: The roles of regulatory factors for muscle regeneration. Cell Biol Int 2017;41(3):228–238; doi: 10.1002/cbin.10705
56. Dort J, Fabre P, Molina T, et al. Macrophages are key regulators of stem cells during skeletal muscle regeneration and diseases. Stem Cells Int 2019;2019:4761427; doi: 10 .1155/2019/4761427
57. de la Durantaye M, Piette AB, van Rooijen N, et al. Macrophage depletion reduces cell proliferation and extracellular matrix accumulation but increases the ultimate tensile strength of injured Achilles tendons. J Orthop Res 2014;32(2):279–285; doi: 10.1002/jor.22504
58. Hays PL, Kawamura S, Deng XH, et al. The role of macrophages in early healing of a tendon graft in a bone tunnel. J Bone Joint Surg Am 2008;90(3):565–579; doi: 10.2106/JBJS.F.00531
59. Sallis RE. Exercise is medicine and physicians need to prescribe it! Med Sport 2009;62(4):517–520.
60. Ohberg L, Lorentzon R, Alfredson H. Eccentric training in patients with chronic Achilles tendinosis: Normalised tendon structure and decreased thickness at follow up. Br J Sports Med 2004;38(1):8–11; discussion 11.
61. Pauly HM, Kelly DJ, Popat KC, et al. Mechanical properties and cellular response of novel electrospun nanofibers for ligament tissue engineering: Effects of orientation and geometry. J Mech Behav Biomed Mater 2016;61:258–270; doi: https://doi.org/10.1016/j.jmbbm.2016.03.022
62. Mohanraj B, Duan G, Peredo A, et al. Mechanically activated microcapsules for ''On-Demand'' drug delivery in dynamically loaded musculoskeletal tissues. Adv Funct Mater 2019;29(15):1807909.
63. Gawri R, Rosenzweig DH, Krock E, et al. High mechanical strain of primary intervertebral disc cells promotes secretion of inflammatory factors associated with disc degeneration and pain. Arthritis Res Ther 2014;16(1):R21; doi: 10 .1186/ar4449
64. Jacobs C, Grimm S, Ziebart T, et al. Osteogenic differentiation of periodontal fibroblasts is dependent on the strength of mechanical strain. Arch Oral Biol 2013;58(7):896–904; doi: https://doi.org/10.1016/j.archoralbio.2013.01.009
65. Lewis JS, Dolgova N, Chancellor T, et al. Dendritic cell activation is influenced by cyclic mechanical strain when cultured on adhesive substrates. Biomaterials 2013;34(36):9063.
66. Baker BM, Chen CS. Deconstructing the third dimension–how 3D culture microenvironments alter cellular cues. J Cell Sci 2012;125(13):3015–3024.
67. Cha B-H, Shin SR, Leijten J, et al. Integrin-mediated interactions control macrophage polarization in 3D hydrogels. Adv Healthc Mater 2017;6(21):1700289; doi: https://doi.org/10.1002/adhm.201700289
68. Lee SWL, Seager RJ, Litvak F, et al. Integrated in silico and 3D in vitro model of macrophage migration in response to physical and chemical factors in the tumor microenvironment. Integrat Biol 2020;12(4):90–108; doi: 10.1093/intbio/zyaa007
69. Li R, Serrano JC, Xing H, et al. Interstitial flow promotes macrophage polarization toward an M2 phenotype. Mol Biol Cell 2018;29(16):1927–1940; doi: 10.1091/mbc.E18-03-0164
70. Soves CP, Miller JD, Begun DL, et al. Megakaryocytes are mechanically responsive and influence osteoblast proliferation and differentiation. Bone 2014;66:111–120; doi: https://doi.org/10.1016/j.bone.2014.05.015
71. Kawata A, Mikuni-Takagaki Y. Mechanotransduction in stretched osteocytes—Temporal expression of immediate early and other genes. Biochem Biophys Res Commun 1998;246(2):404–408; doi: https://doi.org/10.1006/bbrc .1998.8632
72. Peake MA, Cooling LM, Magnay JL, et al. Selected contribution: Regulatory pathways involved in mechanical induction of c-fos gene expression in bone cells. J Appl Physiol 2000;89(6):2498–2507; doi: 10.1152/jappl.2000.89.6.2498
73. Raffa V. Force: A messenger of axon outgrowth. Semin Cell Dev Biol 2023;140:3–12; doi: 10.1016/j.semcdb.2022.07.004
74. Gao G, Ren K, Chen L, et al. Effects of periodic mechanical stress on cytoskeleton dependent lipid raft-induced integrin a1 activation in rat nucleus pulposus cells. J Mol Histol 2023;54(1):67–75; doi: 10.1007/s10735-023-10112-1
75. Tu PC, Pan YL, Liang ZQ, et al. Mechanical stretch promotes macrophage polarization and inflammation via the RhoA-ROCK/NF-kappaB pathway. Biomed Res Int 2022;2022:6871269; doi: 10.1155/2022/6871269

Address correspondence to:
Eda Yildirim-Ayan, PhD
Department of Bioengineering
University of Toledo
2801 W. Bancroft Mail Stop 303
Toledo, OH 43606
USA

E-mail: eda.yildirimayan@utoledo.edu

Received: May 18, 2023
Accepted: September 12, 2023
Online Publication Date: October 27, 2023